

FINAL REPORT

1 General Information

DFG reference number: TS 28/16-1

Project number: 452247553

Project title: Ultrathin coating of fluidized particles by means of aerosol

Name(s) of the applicant(s): Prof. Dr.-Ing. habil. Evangelos Tsotsas

Official address(es): Universitätsplatz 2, 39106 Magdeburg

Name(s) of the co-applicants: –

Name(s) of the cooperation partners: –

Reporting period (entire funding period): 01.10.2021 – 31.12.2024

2 Summary

The primary objective of this project was to conduct an in-depth investigation of a novel and promising particle coating technique utilizing aerosol droplets. To achieve this, fluidized bed coating experiments were carried out under varying process conditions using aerosol droplets with a mean diameter of approximately 1 µm. These experiments aimed to assess the impact of process parameters on key quality attributes such as process yield, coating coverage, and layer thickness. The core materials used in the study were glass and porous γ -Al₂O₃, with mean diameters of 653 µm and 610 µm, respectively. As coating liquids, sodium benzoate (NaB) solution and silicon dioxide (SiO₂) nanosuspension were employed. Following sample collection, scanning electron microscopy (SEM) images of the coated particles were captured and analyzed using MATLAB image processing to evaluate coating coverage while accounting for curvature effects. The obtained coverage data was compared with results from Monte Carlo (MC) simulations. A significant discrepancy was observed due to island growth on the particle surfaces, which can be attributed to the preferential deposition of droplets on pre-coated areas. To improve the accuracy of the coating process simulation, the MC model was modified to incorporate a preferential deposition factor for each experiment. Additionally, some coated particles were cross-sectioned to measure the layer thickness. The intraparticle coating thickness distribution predicted by the MC simulations was found to be in reasonable agreement with the experimentally measured thickness. The findings indicate that process yield, coating coverage,

and the preferential deposition factor are influenced by several experimental parameters, including expanded bed height, fluidization air temperature, atomization pressure, the number of aerosol inlets, and the surface potential of the core particles. Moreover, this study was the first to examine the effect of surface charge on droplet deposition for different core materials, an aspect that was not originally included in the project proposal. In particular, experiments with SiO_2 nanosuspension demonstrated that $\gamma\text{-Al}_2\text{O}_3$ cores could be uniformly coated with SiO_2 nanoparticles, achieving a layer thickness of approximately 1.1 μm . This highlights the potential of aerosol droplet deposition as an innovative semi-wet approach for nanoparticle coating of large particles without the use of binders. Furthermore, a continuum process yield model was developed. Computational fluid dynamics (CFD) simulations were conducted to identify the spray zone within the fluidized bed, enabling the determination of the effective bed height required for yield predictions under different experimental conditions. In future research, integrating this continuum yield model with Monte Carlo deposition simulations may allow for the fully predictive simulation of the coating process, facilitating process optimization and scale up.

Hauptziel dieses Projekts war die eingehende Untersuchung einer neuartigen und vielversprechenden Partikelbeschichtungstechnik unter Verwendung von Aerosoltropfen. Hierfür wurden Beschichtungsexperimente in der Wirbelschicht unter variierenden Prozessbedingungen durchgeführt, wobei Aerosoltropfen von ca. 1 μm verwendet wurden. Die Experimente zielten auf die Auswirkungen der Prozessparameter auf wichtige Qualitätsmerkmale wie Prozessausbeute, Beschichtungsabdeckung und Schichtdicke ab. Die als Kernmaterialien verwendeten Stoffe waren Glas und poröses $\gamma\text{-Al}_2\text{O}_3$ mit mittleren Durchmessern von 653 μm bzw. 610 μm . Als Beschichtungsflüssigkeiten wurden eine Lösung aus Natriumbenzoat (NaB) sowie Nanosuspension aus Siliziumdioxid (SiO_2) eingesetzt. Nach Probenentnahme wurden per Raster-elektronenmikroskopie (REM) Bilder der beschichteten Partikel aufgenommen und per MATLAB analysiert, um die Beschichtungsabdeckung unter Berücksichtigung von Krümmungseffekten auszuwerten. Abdeckungsdaten wurden mit Ergebnissen aus Monte Carlo (MC) Simulationen verglichen. Eine signifikante Abweichung wurde festgestellt, die auf Inselwachstum auf den Partikeloberflächen zurückzuführen ist, als bevorzugte Ablagerung von Tropfen auf bereits beschichteten Bereichen. Um die Genauigkeit der Beschichtungssimulation zu verbessern, wurde das MC Modell um einen Faktor zur bevorzugten Ablagerung erweitert. Zusätzlich wurden einige beschichtete Partikel im Querschnitt analysiert, um die Schichtdicke zu messen. Die durch MC Simulationen vorhergesagte intrapartikuläre Beschichtungsdickenverteilung stimmte recht gut mit der experimentell gemessenen Dicke überein. Die Ergebnisse zeigen,

dass Prozessausbeute, Beschichtungsabdeckung und bevorzugte Ablagerung durch mehrere Prozessparameter beeinflusst werden, darunter expandierte Betthöhe, Temperatur der Fluidisierungsluft, Zerstäubungsdruck, Anzahl der Aerosoleinlässe und das Oberflächenpotenzial der Kernpartikel. Darüber hinaus war diese Studie die erste, die den Einfluss der Oberflächenladung auf die Tropfenablagerung für verschiedene Kernmaterialien untersuchte, ein Aspekt, der ursprünglich nicht im Projektvorschlag enthalten war. Insbesondere zeigten Experimente mit dem SiO_2 -Nanofluid, dass $\gamma\text{-Al}_2\text{O}_3$ Kerne gleichmäßig mit SiO_2 Nanopartikeln beschichtet werden können bei einer Schichtdicke von etwa 1.1 μm . Dies unterstreicht das Potenzial der Aerosoltropfenablagerung als innovativer halbnassen Methode zur Nanopartikelbeschichtung großer Partikel ohne den Einsatz von Bindemitteln. Darüber hinaus wurde ein Kontinuum-Modell für die Prozessausbeute entwickelt. Computational Fluid Dynamics (CFD) Simulationen wurden durchgeführt, um die Sprühzone innerhalb der Wirbelschicht zu identifizieren und die effektive Betthöhe für die Ausbeutevorhersage unter verschiedenen experimentellen Bedingungen zu bestimmen. In zukünftiger Forschung könnte die Integration dieses Modells für die Ausbeute mit MC-Simulationen der Ablagerung eine vollprädiktive Voraussage des Beschichtungsprozesses ermöglichen und somit zur Prozessoptimierung und Skalierung beitragen.

3 Progress Report

Preliminary studies by the applicant had demonstrated the feasibility of aerosol coating of fluidized particles, including the potential of this process to coat with extremely high resolution while using significantly less material compared to conventional spray fluidized bed (SFB) coating. However, these findings were based on a single experiment, evaluated only at a later stage of the process with limited detail. A Monte Carlo model had been employed to analyze the coating evolution over time, but due to its originally simplistic nature and lack of complete validation, its predictive capabilities remained limited. Therefore, this project was the first to conduct an in-depth scientific investigation of aerosol fluidized bed (AFB) coating, combining experimental research with simulations.

3.1 Aerosol fluidized bed experimental setup and experiments

Following a revision of the previous experimental setup, the aerosol inlet tube was redesigned with a serrated structure to prevent liquid films from forming on the inner walls. This modification was necessary to avoid liquid accumulation that could flow into the fluidization chamber and cause clogging at the aerosol inlet. Initially, in preliminary experiments, a longer aerosol inlet tube (145 cm) was used to prevent relatively large droplets from reaching the fluidization chamber. However, to enhance experimental efficiency, the tube length was later reduced to

50 cm, minimizing aerosol droplet loss due to deposition inside the tube during transport. For experiments involving two aerosol inlets, a new fluidization chamber was introduced, along with a second aerosol generator. Further details on these modifications can be found in Akbas et al. (2023) and Akbas et al. (2024).

The influence of six key parameters was examined on coating coverage and process yield. These parameters include fluidized bed height, fluidization air temperature, atomizing air pressure, number of aerosol inlets, type of coating liquid, and core particle material. Additionally, an extended experiment with a 6-hour process duration was conducted to achieve complete particle coverage and enable coating thickness measurements. To assess the coating thickness, individual particles from this extended experiment were halved at their midpoint. Scanning electron microscopy (SEM) images of the equatorial plane were then analyzed using ImageJ to measure the coating layer thickness. A detailed description of the experimental plan and operating conditions can be found in Akbas et al. (2024).

3.2 Monte Carlo model extensions

Adaption of Rieck's Monte Carlo model for use with aerosol

This study built upon the Monte Carlo model introduced by Rieck et al. (2016) for coating with conventional spray in fluidized beds (SFBs). One of the primary challenges in such MC simulations was the excessively long computational time, which reached approximately 16 hours (Mezhericher et al. (2020)), even with only a single particle in the simulation box. This was due to the high number of droplet deposition areas on the surface of the particle, resulting from the small size of aerosol droplets.

A significant improvement was achieved by optimizing the simulation, reducing the computational time to 2.4 hours while accommodating 1000 particles in the simulation box. With this enhanced Monte Carlo model, it became possible to analyze not only intraparticle coating distribution but also the interparticle coating distribution while considering process yield. This advancement marks a significant step in improving the accuracy of Monte Carlo simulations for describing the aerosol fluidized bed (AFB) coating process. Detailed explanations of these improvements were published in Akbas et al. (2023).

Model extension for preferential deposition of droplets on already occupied positions

The Monte Carlo model developed by Rieck et al. (2016) was unable to account for preferential deposition or accurately predict island growth on particle surfaces. To address this limitation, the model was extended in this project to incorporate preferential droplet deposition in Monte Carlo simulations.

When N_d droplets deposit randomly on a particle surface, a fraction AN_d adheres to the already covered part of the surface, while the remaining fraction $(1 - A)N_d$ deposits on unoccupied areas. This relationship is expressed mathematically as:

$$AN_d + (1 - A)N_d = N_d. \quad (1)$$

Analogous to Equation 1, the distribution of in total N_d droplets can be expressed in the case of preferential deposition, where a higher portion of the droplets accumulates on the already coated areas of the particle surface. This division follows the relationship:

$$\left(\frac{x+A}{(x+1)A}\right)AN_d + \left[1 - \left(\frac{x+A}{(x+1)A}\right)A\right]N_d = N_d. \quad (2)$$

The preference x for deposition on already occupied areas is, thus, an input parameter of the MC simulation. The detailed investigation was published and MC simulation steps were explained in Akbas et al. (2023).

3.3 Development of a model for process yield

To develop a continuous model for predicting process yield (i.e., the filtration efficiency of the fluidized bed for aerosol droplets) under varying operating conditions and different surface charges, the approach was based on the continuum particle drying model in fluidized beds proposed by Burgschweiger et al. (1999). In the fluidization chamber three different phases were distinguished: Particles (P), Emulsion Gas (E), and Bubbles (B). The schematic representation of this aerosol bed division is illustrated in Figure 1.

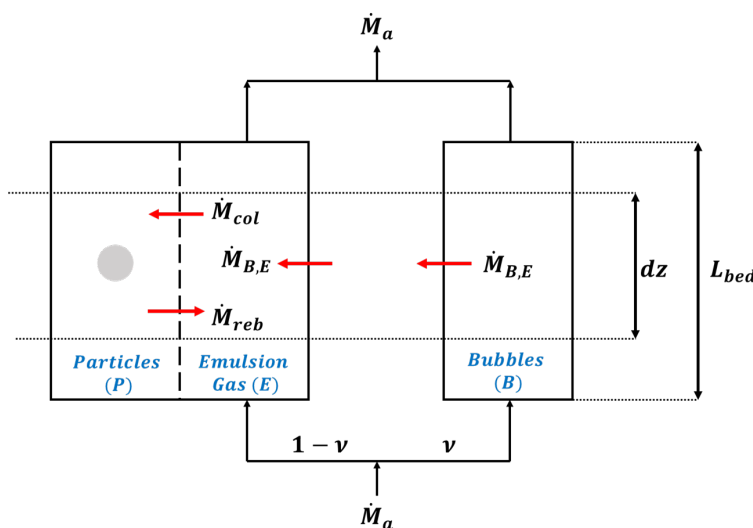


Figure 1: Model scheme of aerosol bed coating.

To develop the process yield model, two mass balance equations for aerosol droplets were formulated; one for the emulsion gas and the other for the bubble phase. The derived balance equation for the emulsion gas is as follows:

$$(1 - v)\dot{M}_a \frac{dX_E}{dz} = \frac{1}{L_{bed}}(\dot{M}_{B,E} + \dot{M}_{reb} - \dot{M}_{col}), \quad (3)$$

where \dot{M}_a is mass flow rate of air, X_E is mass fraction of droplets in the emulsion gas (air flowing through the emulsion phase), $\dot{M}_{B,E}$ is mass flow rate of droplets from bubbles to emulsion phase, \dot{M}_{reb} is mass flow rate of droplets which rebound from particle surfaces, \dot{M}_{col} is mass flow rate of droplets which collide with particles, and L_{bed} is bed height.

The respective balance equation for the bubble phase is as follows:

$$v\dot{M}_a \frac{dX_B}{dz} = \frac{1}{L_{bed}}(-\dot{M}_{B,E}), \quad (4)$$

where X_B is mass fraction of droplets in bubble phase.

After complementing the mass balance equations with kinetics from filtration theory for the mass flow rates of aerosol droplets that collide with the fluidized particles and rebound from/adhere to them, MATLAB was used to solve the equations under the corresponding experimental conditions for each experiment, to predict process yields.

Bed height (L_{bed}) is a critical input parameter for the process yield model. If the aerosol were evenly distributed throughout the entire bed, the total bed height could be used in the model. However, in this study, since the aerosol was introduced from the side of the fluidization chamber, the relevant bed height for the yield model corresponds to the volume of the aerosol affected part of the bed (spray zone) rather than the total bed volume.

To assess the aerosol distribution within the fluidized bed and identify the spray zone, computational fluid dynamics (CFD) simulations were performed for each experiment under their respective conditions. Droplet deposition is not considered in those simulations, so that the size of the aerosol-affected areas is obtained from the expansion of aerosol-containing air flows, introduced from one or two sides in the fluidization chamber. As an example, the aerosol-flow distribution contours for two experiments are shown in Figure 2.

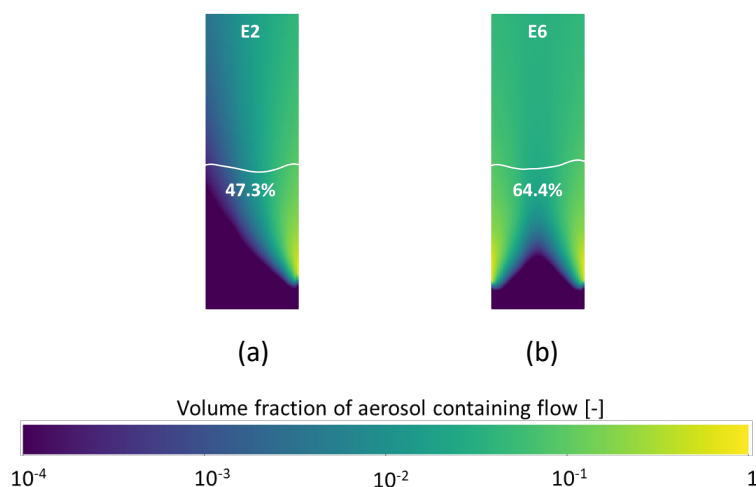


Figure 2: Distribution of volume fraction of aerosol containing flow in the fluidized bed (a) for one aerosol inlet, (b) for two aerosol inlets with otherwise same experimental conditions (white line represents the total bed height)

As shown in Figure 2, increasing the number of inlets to two resulted in an expansion of the so-called spray zone (from 47.3% to 64.4% of the total bed volume). Based on CFD simulations, both the spray zone (where aerosol droplets can deposit on particles) and the effective bed height can be determined for each experiment and incorporated into the one-dimensional process yield model. Additionally, the influence of various process conditions on the spray zone can be systematically analyzed. Results from the CFD simulations about the extent of the spray zone under different process conditions, as well as results from the process yield model have been obtained, and manuscripts are currently being prepared for publication.

3.4 Results and Discussion

Process yields

The experiments conducted with $\gamma\text{-Al}_2\text{O}_3$ core particles resulted in higher process yields compared to those using glass core particles. Several factors contribute to this difference, each of which has been analyzed in detail under various process conditions in Akbas et al. (2024).

Preferences obtained from Monte Carlo simulations

The preference values, and consequently island growth, were found to be influenced by experimental conditions. Certain changes in process parameters promote increased island growth due to more preferential droplet deposition, while others reduce it. Additionally, the extent of island growth varies depending on the type of core material, which in this study included glass and $\gamma\text{-Al}_2\text{O}_3$. A detailed analysis of the obtained preference values, along with the effects of changing conditions on island growth, is provided in Akbas et al. (2024).

Zeta potential effect on coating for different cores

During coating experiments with fresh $\gamma\text{-Al}_2\text{O}_3$ cores, SEM images revealed that the particle surfaces exhibited minimal coating. This was unexpected because of their surface roughness which should have facilitated better coverage. Additionally, a storage issue was observed with

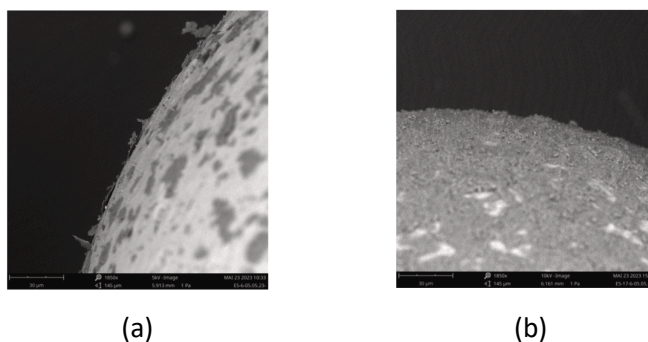


Figure 3: SEM pictures of the surfaces of coated particles after 2 weeks of storage, scale bars: 30 μm (a) originally fresh $\gamma\text{-Al}_2\text{O}_3$ particle (b) glass particle

coated $\gamma\text{-Al}_2\text{O}_3$ particles, as the coating gradually detached from the surface over time, as shown in Figure 3a. In contrast, no such detachment occurred on coated glass particles (Figure

3b). This observation further reinforced the hypothesis that differences in surface charge between the core materials played a significant role in aerosol coating.

Zeta potential measurements of glass and fresh γ -Al₂O₃ cores confirmed that the observed differences in coating behavior were due to variations in surface potential. Additional experiments with mixed core materials further supported this finding. Specifically, glass particles exhibited a negative surface potential, whereas fresh γ -Al₂O₃ particles had a positive surface potential. A detailed discussion of these findings is provided in Akbas et al. (2024).

Another challenge with γ -Al₂O₃ particles was accurately measuring the process yield. To address this issue, fresh γ -Al₂O₃ particles were washed with distilled water, and the coating experiment was repeated using these washed particles. The results clearly showed that after the hydration process, more coating was retained on the particle surfaces. This was attributed to surface modifications caused by hydration products, which reduced the positive surface potential of γ -Al₂O₃. As a result, aerosol droplet deposition was more effective on washed γ -Al₂O₃ particles compared to fresh ones, and process yield measurement was much easier. Consequently, all subsequent experiments with γ -Al₂O₃ were conducted using washed particles. A detailed analysis of these findings is published in Akbas et al. (2024).

Coating thickness evaluation of particles coated with NaB

Analysis of cut particle images from the 6-hour experiment revealed that the island growth effect from the early coating stages remained a significant factor for the uniformity of intraparticle coating thickness (Figure 4). The intraparticle coating thickness distribution predicted by Monte Carlo simulations showed a reasonable match with the measured thickness from the cut particles. A detailed discussion of these results is provided in Akbas et al. (2024).

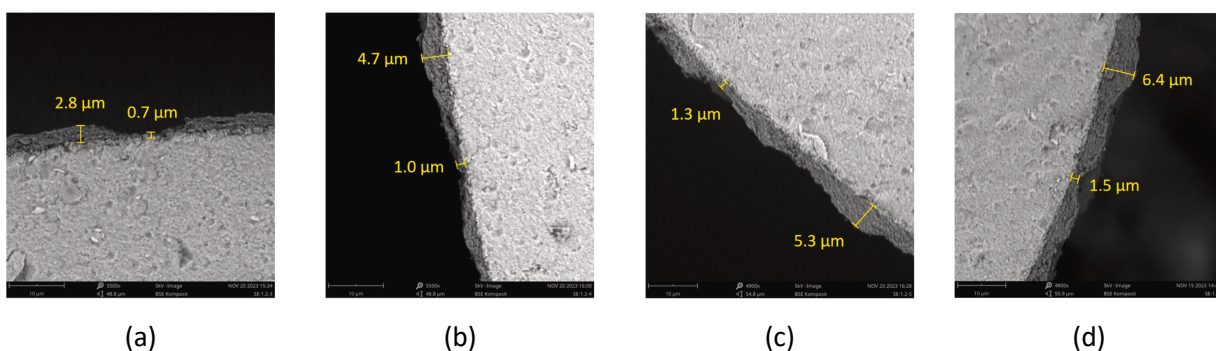


Figure 4: Wavy structure of NaB coating layer on γ -Al₂O₃ particle after (a) 3 h, (b) 4 h, (c) 5 h, (d) 6 h of process time. Scale bars: 10 μ m.

Coating thickness evaluation of particles coated with SiO₂ nanosuspension

A key observation was that the coating structure obtained with SiO₂ nanosuspension differed from that with NaB. More SiO₂ nanoparticle clusters were detected on γ -Al₂O₃ particles compared to glass particles, which is an opposite situation to the NaB coating. This variation can

be attributed to the surface potential differences among glass, $\gamma\text{-Al}_2\text{O}_3$ cores, and SiO_2 nanoparticles. A detailed investigation of this phenomenon is provided in Akbas et al. (2024). The thickness of the SiO_2 coating was measured by sectioning $\gamma\text{-Al}_2\text{O}_3$ particles at the end of the experiment. Figure 5 presents an SEM image of the SiO_2 coating structure.

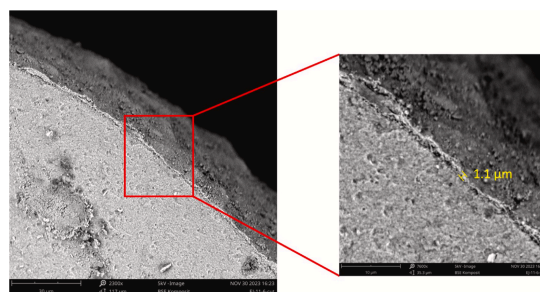


Figure 5: Structure of the SiO_2 nanoparticle coating layer on a $\gamma\text{-Al}_2\text{O}_3$ particle. Scale bars: 30 μm , 10 μm .

In general, SiO_2 nanoparticle coating was significantly more uniform than the NaB coating. This difference can be attributed to the mobility of SiO_2 nanoparticles under the influence of surface charge forces after drying, unlike NaB . The measured coating thickness was approximately 1.1 μm , which is considered ultrathin in absolute terms. Relative to the nanoparticle size, this corresponds to 50 particle layers, given the mean diameter of SiO_2 nanoparticles is 22 nm. A detailed analysis of these findings is provided in Akbas et al. (2024).

Bibliography

Akbas, S., Chen, K., Hoffmann, T., Scheffler, F., and Tsotsas, E. (2023). Investigation of island growth on fluidized particles coated by means of aerosol. In: *Processes* 11, 165. doi: 10.3390/pr11010165.

Akbas, S., Zhang, J., Hoffmann, T., and Tsotsas, E. (2024). Aerosol fluidized bed coating: Exploring the impact of process conditions on process yield, coating coverage and thickness. In: *Chemical Engineering Journal* 495, 153349. doi: 10.1016/j.cej.2024.153349.

Burgschweiger, J., Groenewold, H., Hirschmann, C., and Tsotsas, E. (1999). From hygroscopic single particle to batch fluidized bed drying kinetics. In: *The Canadian Journal of Chemical Engineering* 77, S. 333–341. doi: 10.1002/cjce.5450770218.

Mezhericher, M., Rieck, C., Razorenov, N., and Tsotsas, E. (2020). Ultrathin coating of particles in fluidized bed using submicron droplet aerosol. In: *Particuology* 52, S. 78–85. doi: 10.1016/j.partic.2020.03.005.

Rieck, C., Bück, A., and Tsotsas, E. (2016). Monte Carlo modeling of fluidized bed coating and layering processes. In: *AIChE Journal* 62.8, S. 2670–2680. doi: 10.1002/aic.15237.

4 Published Project Results

4.1 Publications with scientific quality assurance

Akbas, S.; Chen, K.; Hoffmann, T.; Scheffler, F.; Tsotsas, E. (2023): Investigation of island growth on fluidized particles coated by means of aerosol. In: *Processes* 2023, 11, 165. DOI: 10.3390/pr11010165

Akbas, S.; Hoffmann, T.; Chen, K.; Scheffler, F.; Tsotsas, E. (2023): Investigation of island growth on particles coated by means of aerosol. In: *Proceedings of the 10th International Granulation Workshop*. Sheffield, UK, 21-23 June 2023.

Akbas, S.; Zhang, J.; Hoffmann, T.; Tsotsas, E. (2024): Aerosol fluidized bed coating: Exploring the impact of process conditions on process yield, coating coverage and thickness. In: *Chemical Engineering Journal*, 495, 153349. DOI: 10.1016/j.cej.2024.153349

Akbas, S.; Hoffmann, T.; Tsotsas, E. (2024): Ultrathin aerosol coating process for fluidized particles. In: *Proceedings of the 23rd International Drying Symposium (IDS2024)*. Wuxi, Jiangsu Province, China, 22-25 November, 2024.

4.2 Other publications and published results

Akbas, S.; Hoffmann, T.; Tsotsas, E. (2022): Ultrathin coating of fluidized particles by means of aerosol. Poster Presentation *Jahrestreffen 2022 der DECHEMA-Fachgruppen Lebensmittelverfahrenstechnik (LVT) und Trocknungstechnik (TRO)*. Frankfurt am Main, Germany, 10-11 March 2022.

Akbas, S.; Hoffmann, T.; Chen, K.; Scheffler, F.; Tsotsas, E. (2023): Investigation of island growth on particles coated by means of aerosol. Poster Presentation *Jahrestreffen 2023 der DECHEMA-Fachgruppen Abfallbehandlung und Wertstoffrückgewinnung (AuW) und Trocknungstechnik (TRO)*. Dresden, Germany, 6-7 March 2023.

Akbas, S.; Hoffmann, T.; Tsotsas, E. (2023): Ultrathin particle coating in fluidized bed by using aerosols. Poster Presentation *International Congress on Particle Technology (PARTEC)*. Nuremberg, Germany, 26-28 September 2023.

Akbas, S.; Hoffmann, T.; Tsotsas, E. (2024): Exploring the impact of process conditions on aerosol coating quality and coverage. Oral Presentation *Jahrestreffen 2024 der DECHEMA-Fachgruppen Wärme- und Stoffübertragung (WSUE) und Trocknungstechnik (TRO)*. Magdeburg, Germany, 11-13 March, 2024.

Akbas, S.; Mezhericher, M.; Hoffmann, T.; Razorenov. N; Pan. Z; Tsotsas, E. (2025): Fine-tuning particle coatings: A comparative study of liquid atomization methods in fluidized bed processes. DOI: <https://doi.org/10.5281/zenodo.15632360>

4.3 Patents (applied for and granted)